2015 International Symposium on Nonlinear Theory and its Applications
NOLTA2015, Kowloon, Hong Kong, China, December 1-4, 2015

Reconstruction of Bifurcation Diagrams with Lyapunov Exponents for Chaotic Systems from only Time-series Data

Yoshitaka Itoh†, Yuta Tada‡ and Masaharu Adachi§

Department of Electrical and Electronic Engineering, Tokyo Denki University
5 Senju-Asahicho Adachi-ku, Tokyo 210-8551, Japan
Email: †15ky001@ms.dendai.ac.jp, ‡13kme33@ms.dendai.ac.jp, §adachi@eee.dendai.ac.jp

Abstract—We describe the reconstruction of bifurcation diagrams with Lyapunov exponents for chaotic systems using only data from several time-series. The algorithm, which was originally proposed by Tokunaga *et al.*, for reconstructing a bifurcation diagram with the corresponding Lyapunov exponents is as follows. First, we model a dynamical system of several time-series by a time-series predictor. In this paper, an extreme learning machine is used as the time-series predictor. Next, we estimate the number of significant parameters of the target dynamical system from the modeled dynamical system by principal component analysis. Then, we reconstruct the bifurcation diagrams with the Lyapunov exponents of the target dynamical system. We show the results of numerical experiments on the reconstruction of bifurcation diagrams with Lyapunov exponents for the logistic and Hénon maps.

1. Introduction

The estimation of Lyapunov exponents is one of several important methods used for the analysis of chaotic systems. However, the targets of analysis among chaotic systems were limited to only known systems.

Tokunaga *et al.* [1] have proposed reconstructing bifurcation diagrams from time-series data alone. This method estimates the number of significant parameters and reconstructs bifurcation diagrams of unknown systems. We have proposed using extreme learning machines (ELMs) to reconstruct bifurcation diagrams [2, 3] because the computation time of this method is shorter than that of the conventional method used by Tokunaga *et al.*. ELM is not only the computation time is shorter but the prediction accuracy also is higher for single time-series data.

In this paper, we estimate the Lyapunov exponents for an unknown chaotic system using only the data of several series [4, 5, 6].

2. Time-series Predictor

The reconstruction of the bifurcation diagram of a dynamical system uses the time-series predictor

$$\mathbf{y}(t+1) = G(\mathbf{w}, \mathbf{y}(t)) \tag{1}$$

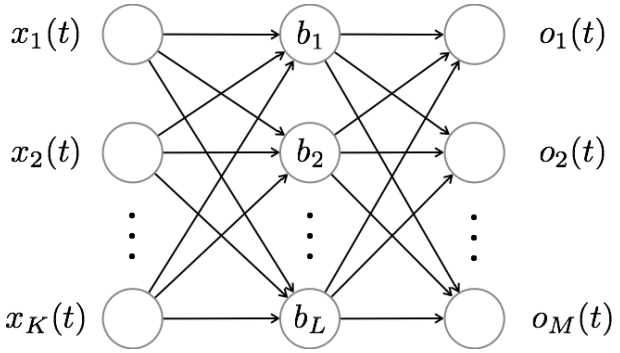

Figure 1: Structure of ELM.

where $G(\cdot)$ is a nonlinear function, $\mathbf{y}(t)$ and $\mathbf{y}(t+1)$ are the time-series to be predicted and the input and output of the predictor, and $\mathbf{w}$ is learned connection weights.

In this paper, we use an ELM as the time-series predictor. The ELM is a three-layer feed-forward neural network with the structure shown in Fig. 1. The output of the lth hidden neuron h_l is

$$h_l(t) = f\left(\sum_{k=1}^{K} w_{lk}^{(h)} x_k(t) + b_l\right) \tag{2}$$

where $w_{lk}^{(h)}$ denotes the hidden weight from the kth input neuron to the lth hidden neuron, b_l is the bias of the lth hidden neuron, and $f(\cdot)$ is the sigmoid function. The output of the mth output neuron o_m is

$$o_m(t) = \sum_{l=1}^{L} w_{ml}^{(o)} h_l(t) \tag{3}$$

where $w_{ml}^{(o)}$ denotes the output weight from the lth hidden neuron to the mth output neuron. In this paper, the number of output neurons M is set to be equal to the number of input neurons K: that is, $M = K$. These numbers M and K are set to be equal to the target dynamical system. $W^{(o)}$ is obtained by the following linear regression for learning in this model.

$$W^{(o)} = \left(H^{-1}D\right)^T \tag{4}$$

Here, T indicates transposition and H^{-1} is the pseudo-inverse matrix of H. The matrices H, D and $W^{(0)}$ are given

by

$$H = \begin{bmatrix} h_1(1) & \cdots & h_L(1) \\ \vdots & \ddots & \vdots \\ h_1(N) & \cdots & h_L(N) \end{bmatrix}, \tag{5}$$

$$D = \begin{bmatrix} d_1(1) & \cdots & d_M(1) \\ \vdots & \ddots & \vdots \\ d_1(N) & \cdots & d_M(N) \end{bmatrix}, \tag{6}$$

$$W^{(o)} = \begin{bmatrix} w^{(o)}_{1,1} & \cdots & w^{(o)}_{M,1} \\ \vdots & \ddots & \vdots \\ w^{(o)}_{1,L} & \cdots & w^{(o)}_{M,L} \end{bmatrix}. \tag{7}$$

3. Reconstruction of Bifurcation Diagrams

In this section, we describe the method for reconstruction of bifurcation diagrams using only time-series data. We assume that the time-series data are generated by one system and that this target system can be represented by a smooth mapping of N points in a parameter space $P = [p(1), \cdots, p(N)]$.

First, each set of time-series data is modeled by the ELM. The output weights $[\mathbf{w^{(o)}}(1), \mathbf{w^{(o)}}(2), \cdots, \mathbf{w^{(o)}}(N)]$ corresponding to parameters $[p(1), p(2), \cdots, p(N)]$ are obtained from Eq. (4). If the number of output neurons is more than two, the output weight matrix becomes

$$\begin{bmatrix} \mathbf{w^{(o)}}(1) \\ \vdots \\ \mathbf{w^{(o)}}(N) \end{bmatrix}^T = \begin{bmatrix} w^{(o)}_{1,1}(1) & \cdots & w^{(o)}_{1,1}(N) \\ w^{(o)}_{1,2}(1) & \cdots & w^{(o)}_{1,2}(N) \\ \vdots & \ddots & \vdots \\ w^{(o)}_{1,L}(1) & \cdots & w^{(o)}_{1,L}(N) \\ w^{(o)}_{2,1}(1) & \cdots & w^{(o)}_{2,1}(N) \\ \vdots & \ddots & \vdots \\ w^{(o)}_{M,L}(1) & \cdots & w^{(o)}_{M,L}(N) \end{bmatrix}. \tag{8}$$

Next, we estimate a low-dimensional space of the output weights by using principal component analysis. A variance–covariance matrix Ω is constructed from the output weights of Eq. (8):

$$\Omega = \begin{bmatrix} var(\delta\mathbf{w^{(o)}}(1)) & \cdots & cov(\delta\mathbf{w^{(o)}}(1), \delta\mathbf{w^{(o)}}(N)) \\ \vdots & \ddots & \vdots \\ cov(\delta\mathbf{w^{(o)}}(N), \delta\mathbf{w^{(o)}}(1)) & \cdots & var(\delta\mathbf{w^{(o)}}(1)) \end{bmatrix} \tag{9}$$

where $var(\cdot)$ and $cov(\cdot, \cdot)$ denote variance and covariance, respectively, and $\delta\mathbf{w^{(o)}}(n)$ is given by

$$\delta\mathbf{w^{(o)}}(n) = \mathbf{w^{(o)}}(n) - \mathbf{w^{(o)}_0} \ \ (n = 1, \cdots, N) \tag{10}$$

with

$$\mathbf{w^{(o)}_0} = \frac{1}{N} \sum_{n=1}^{N} \mathbf{w^{(o)}}(n). \tag{11}$$

We obtain the eigenvalues and eigenvectors of Ω by eigenvalue decomposition. The eigenvalues are arranged in descending order

$$\lambda_1 \geq \lambda_2 \geq \cdots \geq \lambda_N. \tag{12}$$

and the eigenvectors corresponding to eigenvalue λ_i is denoted $\mathbf{u_i}$. Then, $\delta\mathbf{w}_{(o)}$ is determined by using the principal component coefficients $\Gamma = [\gamma_1, \gamma_2, \cdots, \gamma_D]$ and the eigenvectors:

$$\delta\mathbf{w^{(o)}} = [\mathbf{u_1}, \mathbf{u_2}, \cdots, \mathbf{u_N}]\Gamma \tag{13}$$

where

$$\Gamma = [\mathbf{u_1}, \mathbf{u_2}, \cdots, \mathbf{u_N}]^{-1} \delta\mathbf{w^{(o)}}. \tag{14}$$

Next, we determine the optimal dimension for $\delta\mathbf{w^{(o)}}$ from the eigenvalues. The contribution ratio E of the qth principal component and the cumulative contribution ratio CE to λ_q from λ_1 can be obtained from the following equations:

$$E = \frac{\lambda_q}{\sum_{i=1}^{D} \lambda_i} \times 100[\%], \tag{15}$$

$$CE = \frac{\sum_{q=1}^{Q} \lambda_q}{\sum_{i=1}^{D} \lambda_i} \times 100[\%]. \tag{16}$$

We define a bifurcation path to be a sequence of points $(p(1) \to p(2) \to \cdots \to p(J))$ in the parameter space of the target system and a bifurcation locus to be a sequence of points $\left(\gamma^{(C)}(1) \to \gamma^{(C)}(2) \to \cdots \to \gamma^{(C)}(J)\right)$ in the space of the principal component coefficients. If the relations between the points in the bifurcation locus are preserved in the bifurcation paths, then we can determine the space of principal component coefficients that duplicates the parameter space of the target system.

By adding $\mathbf{w_0^{(o)}}$ to Eq. (13), a new output vector that can be used in the reconstruction of the bifurcation diagram is obtained

$$\tilde{\mathbf{w}}^{(\mathbf{o})} = [\mathbf{u_1}, \mathbf{u_2}, \cdots, \mathbf{u_N}] \begin{bmatrix} \gamma^{(C)} \\ \mathbf{0} \end{bmatrix} + \mathbf{w_0^{(o)}}. \tag{17}$$

The nonlinear map for the reconstruction of the bifurcation diagram is then

$$\mathbf{y}(t+1) = G\left(\tilde{\mathbf{w}}^{(\mathbf{o})}, \mathbf{y}(t)\right). \tag{18}$$

4. Estimation of Lyapunov Exponents using Obtained Nonlinear Map

We estimate the Lyapunov exponents using the obtained nonlinear map[4, 5, 6]. The algorithm is as follows.

First, the Jacobian matrix of the nonlinear map $G(\cdot)$ in Eq. (18) is decomposed by QR decomposition.

$$JG\left(\tilde{\mathbf{w}}^{(\mathbf{o})}, \mathbf{y}(t)\right) Q_t = Q_{t+1} R_{t+1} \ \ (t = 0, \cdots, T) \tag{19}$$

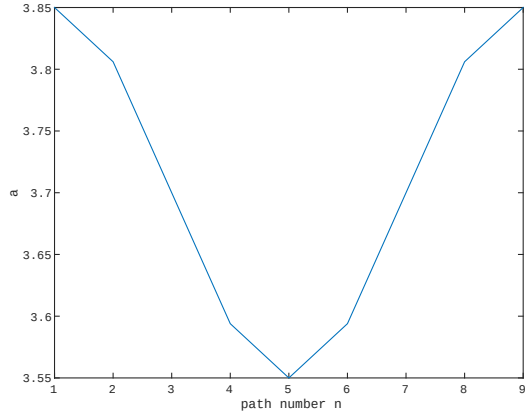

Figure 2: Bifurcation path of the logistic map.

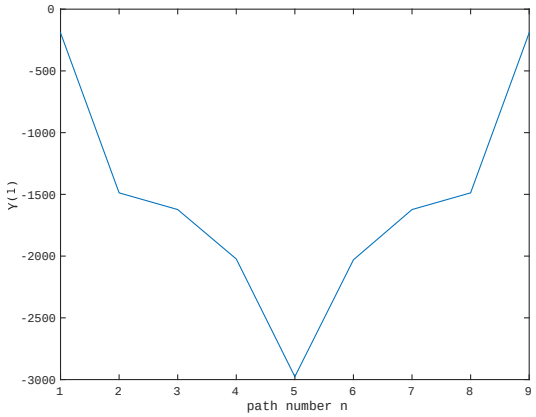

Figure 3: Bifurcation locus of the logistic map.

Here, Q is an orthogonal matrix (Q_0 is the identity matrix), R is an upper triangular matrix and

$$JG\left(\tilde{\mathbf{w}}^{(\mathbf{o})}, \mathbf{y}(t)\right) = \begin{bmatrix} \frac{\partial G(\tilde{\mathbf{w}}_1^{(\mathbf{o})}, \mathbf{y}(\mathbf{t}))}{\partial y_1(t)} & \cdots & \frac{\partial G(\tilde{\mathbf{w}}_1^{(\mathbf{o})}, \mathbf{y}(\mathbf{t}))}{\partial y_K(t)} \\ \vdots & \ddots & \vdots \\ \frac{\partial G(\tilde{\mathbf{w}}_M^{(\mathbf{o})}, \mathbf{y}(\mathbf{t}))}{\partial y_1(t)} & \cdots & \frac{\partial G(\tilde{\mathbf{w}}_M^{(\mathbf{o})}, \mathbf{y}(\mathbf{t}))}{\partial y_K(t)} \end{bmatrix}. \quad (20)$$

The Lyapunov exponents are obtained using the solution of Eq.(19):

$$\mu_i = \lim_{T\to\infty} \frac{1}{T} \sum_{t=1}^{T} \log r_{ii}(t) \ \ (i = 1, \cdots, M) \quad (21)$$

where $r_{ii}(t)$ is the ith diagonal component of R_t.

5. Numerical Experiments

In this section, we show the results of reconstructions of bifurcation diagrams with Lyapunov exponents for the logistic and Hénon maps.

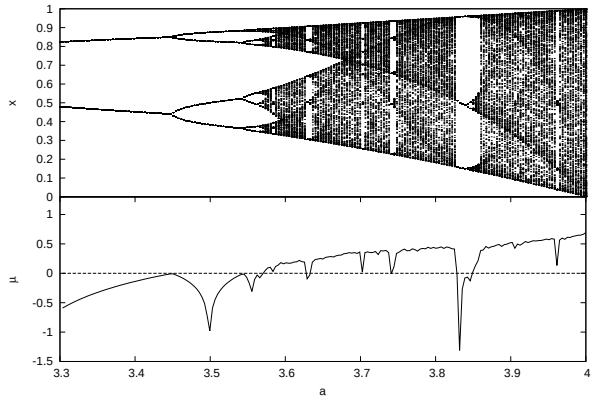

Figure 4: Original bifurcation diagram with Lyapunov exponents of the logistic map.

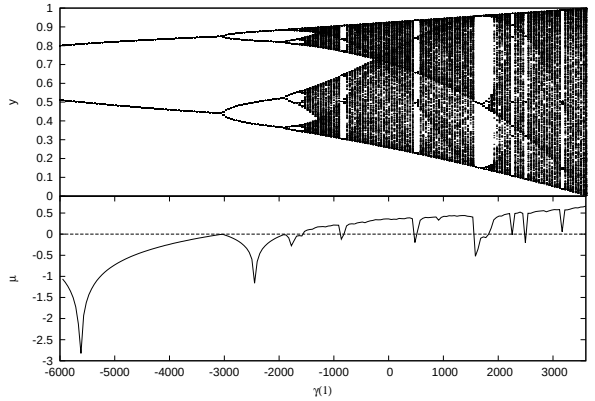

Figure 5: Reconstructed bifurcation diagram with Lyapunov exponents of the logistic map.

5.1. Logistic Map

The logistic map, represented by

$$x(t+1) = ax(t)\left(1 - x(t)\right), \quad (22)$$

has one parameter, a. We generated time-series data for a 9-tuple of parameter values of a determined by

$$a_i = 0.15\cos\left(2\pi(i-1)/8\right) + 3.7 \ (i = 1, \cdots, L = 9). \quad (23)$$

The bifurcation path is shown in Fig. 2. In the training process, we set the number of input neurons, hidden neurons and output neurons to 1, 15, and 1, respectively. The length of the training data for each value of a was 1000. Figure 3 shows the bifurcation locus. The relation between points in Fig. 3 are preserved in Fig. 2, so the space of the principal component coefficients is an approximation to the target parameter space.

Figures 4 and 5 show, respectively, the original and reconstructed bifurcation diagrams with Lyapunov exponents. In Fig. 5, the Lyapunov exponent is negative in periodic oscillation regions and is close to zero at the points of

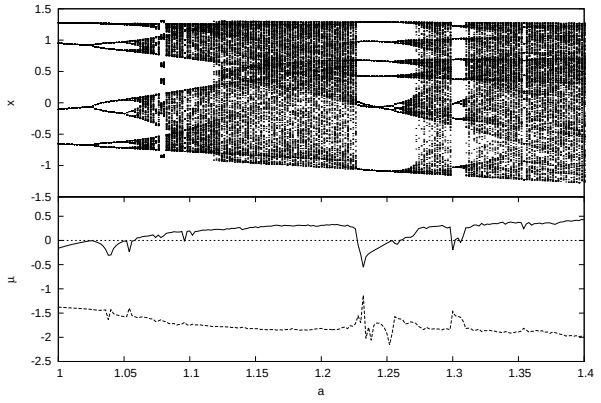

Figure 6: Original bifurcation diagram with Lyapunov exponents of the Hénon map.

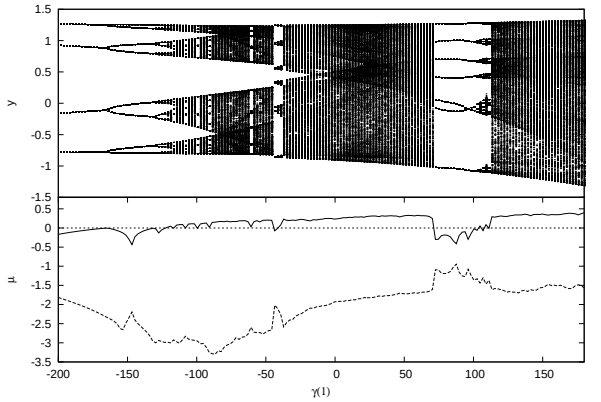

Figure 7: Reconstructed bifurcation diagram with Lyapunov exponents of the Hénon map.

a period-doubling bifurcation. Furthermore, the Lyapunov exponent in chaotic regions is positive. These results show that the bifurcation diagram with Lyapunov exponent was successfully reconstructed because they qualitatively coinside.

5.2. Hénon Map

The Hénon map, represented by

$$x(t+1) = y(t) + 1 - ax^2(t), \tag{24}$$

$$y(t+1) = bx(t), \tag{25}$$

has two parameters, a and b. However, in this paper we are considering the reconstruction of only one-parameter bifurcation diagrams, so b is fixed at 0.3. We generated time-series data for a 9-tuple of parameters values of a determined by

$$a_i = 0.2\cos(2\pi(i-1)/8) + 1.2 \ (i = 0, \cdots, L = 9). \tag{26}$$

In the training process, we set the number of input neurons, hidden neurons and output neurons to 2, 10, and 2, respectively. The length of the training data for each value of a was 1000.

Figures 6 and 7 show, respectively, the original and reconstructed bifurcation diagrams with Lyapunov exponents. In these figures, the solid and dashed lines show the first and second Lyapunov exponents, respectively. These figures show that the bifurcation diagram with Lyapunov exponent of the Hénon map was also successfully reconstructed because they qualitatively coinside.

6. Conclusion

In this paper, we have reconstructed bifurcation diagrams with Lyapunov exponents for the logistic and Hénon maps by using an ELM. The results of simulation experiments show successful reconstruction of bifurcation diagrams with corresponding Lyapunov exponents.

In future work, we will try to estimate other indices for chaotic systems through the reconstruction of bifurcation diagrams from time-series data.

Acknowledgments

The authors would like to thank anonymous reviewers for their fruitful suggestions and comments.

References

[1] R. Tokunaga, S. Kajiwara and S. Matsumoto, "Reconstructing bifurcation diagrams only from time-waveforms," *Physica D*, vol.79, pp.348–360, 1994.

[2] Y. Tada and M. Adachi, "Reconstruction of Bifurcation Diagrams Using Extreme Learning Machines," *2013 IEEE International Conference on Systems, Man, and Cybermetics*, vol.79, pp.1127–1131, 2013.

[3] G.B. Huang, Q.Y. Zhu and C.K. Siew, "Extreme Learning Machine:Theory and Applications," *Neurocomputing*, vol.70, pp.489–501, 2006.

[4] Shimada, I. and Nagashima, T., "A numerical approach to ergodic problem of dissipative dynamical systems," *Prog. Theor. Phys.*, vol.61, no.6, pp.1605–1616, 1979.

[5] M. Sano and Y. Sawada, "Measurement of the Lyapunov Spectrum from Chaotic Time Series," *Phys. Rev. Lett.*, vol.55, 1985.

[6] M.Adachi and M.Kotani, "Identification of Chaotic Dynamical Systems with Back-Propagation Neural Networks," *IEICE Trans. Fundamentals*, vol.E77-A, No.1, 1994.